

SURVEY AND SUMMARY

Monitoring the spatio-temporal organization and dynamics of the genome

Haitham A. Shaban^{1,2,*} and Andrew Seeber^{1,*}

¹Center for Advanced Imaging, Harvard University, Cambridge, MA 02138, USA and ²Spectroscopy Department, Physics Division, National Research Centre, Dokki, 12622 Cairo, Egypt

Received November 30, 2019; Revised February 17, 2020; Editorial Decision February 18, 2020; Accepted February 23, 2020

ABSTRACT

The spatio-temporal organization of chromatin in the eukaryotic cell nucleus is of vital importance for transcription, DNA replication and genome maintenance. Each of these activities is tightly regulated in both time and space. While we have a good understanding of chromatin organization in space, for example in fixed snapshots as a result of techniques like FISH and Hi-C, little is known about chromatin dynamics in living cells. The rapid development of flexible genomic loci imaging approaches can address fundamental questions on chromatin dynamics in a range of model organisms. Moreover, it is now possible to visualize not only single genomic loci but the whole genome simultaneously. These advances have opened many doors leading to insight into several nuclear processes including transcription and DNA repair. In this review, we discuss new chromatin imaging methods and how they have been applied to study transcription.

INTRODUCTION

The spatio-temporal organization of chromatin in the eukaryotic cell nucleus is of vital importance for transcription, DNA replication and genome maintenance (1–7). Each of these activities is tightly regulated in both time and space, for example, DNA replication occurs during the S phase of the cell cycle, initiating at discrete points in the genome (4,5). Another example is the repair of DNA double-strand breaks (DSBs), where the genomic position of a lesion, as well as the cell cycle stage contribute to the decision of which molecular pathway is used to repair the break (6,7). Decades of research revealed that chromatin in the nucleus is not uniformly distributed but rather compartmentalized

(8,9). The organization of the genome varies at different temporal scales as well. For example from HiC data, chromosome structures of 0.1 Mb show dynamics with a fast relaxation time of a few seconds (1–10 s), while the spatial organization of the entire chromosome is slower (10). Another example from live cell imaging of DNA DSB dynamics in budding yeast showed that the spatial chromatin organization differ at various time scales (11,12). Therefore, it is important to understand not only how chromatin is organized spatially but also over time.

Much work now goes into linking the structure and organization of chromatin in the nucleus to the above-mentioned biological functions. However, even in cases where the ‘topography’ of one of these nuclear processes is known, its temporal dynamics are often ill defined (13–16). Dynamics, however, are hugely important. A variety of proteins, including transcription factors, must search the nucleus to find their DNA targets, a process that can either be hindered or facilitated by chromatin structure (17–20). Other prominent examples exist: the formation of chromatin domains by loop extrusion is a dynamic process (21–24), and integration of DNA sequences into the genome using homology directed repair, requires the donor DNA to interact with the site of insertion (25,26). For many of these processes, some degree of chromatin movement is necessary. However, it is unclear if changes in dynamics facilitate biological processes or whether the observed changes are simply consequences. For example, relocation of replication origins to the nuclear interior of budding yeast is associated with an increase in their mobility (27). Does this change in mobility facilitate replication by increasing the chance that an origin moves to a ‘replication center’? Or does it simply reflect a detachment from the nuclear periphery with no additional function? Future work employing gain-of-function assays will be necessary to better link changes in dynamics to function.

*To whom correspondence should be addressed. Tel: +1 617 496 0993; Email: aseeber@fas.harvard.edu
Correspondence may also be addressed to Haitham A. Shaban. Email: h.shaban@aucegypt.edu

Our understanding of chromatin in terms of structure has increased exponentially since the invention of chromatin capture technologies culminating in Hi-C (28–31). Single cell Hi-C and the development of techniques to visualize whole chromatin domains in fixed cells, such as FISH, will undoubtedly lead to a robust understanding of how the genome is organized in all its configurations (32–41). However, without understanding the dynamics of all components involved in these nuclear processes, our insight into how these components interact will always be limited. It is true that inferences about dynamics can be made from enough single cell Hi-C or imaging data, but these inferences will need to be confirmed experimentally requiring assays that can monitor dynamics in living cells. However, a lack of appropriate tools had until recently restricted the study of the space-time organization of chromatin. New methods have overcome this and can visualize chromatin in living cells, with nanometer (42,43) and sub-second resolution (43). In the next section of this review, we highlight these imaging techniques.

LIVE CELL CHROMATIN IMAGING

Visualizing DNA in living eukaryotic cells

Specific genomic loci were initially visualized with the binding of a monomeric GFP–Lac repression fusion protein to integrated lac operator (LacO) arrays at target loci (44,45) (Figure 1A). Multi-locus imaging was later enabled with the similar development of the Tet repressor–Tet (TetO) operator system (46). These systems provided a plethora of information on the dynamics of specific chromatin loci in living cells (6,47). While powerful, these initial systems required that an approximately 10 kb repressor array be integrated into the genome at the locus of interest. Thus, these systems saw far greater use in cells where DNA could be readily inserted into the genome, such as budding yeast. Until relatively recently, fluorescent zinc finger proteins or transcription activator-like effectors (TALEs) were used to visualize specific genomic loci (Figure 1B). However, the drawback is that these proteins must be custom produced for each locus targeted (6). A sea change came with the innovation of the CRISPR (clustered regularly interspaced short palindromic repeat)–Cas9 (CRISPR-associated protein 9) system (48) (Figure 1C). Fluorescently tagged, catalytically dead Cas9 enzymes (dCas9) or modified single guide RNAs (sgRNAs) that recruit fluorescent molecules are now widely used to target specific genomic loci in living cells (26,47,49–58). dCas9 systems are flexible because only the sgRNA must be changed to target a different locus, which is a major advantage over other visualization methods. Cas9 based imaging approaches have now even been used to monitor the motion of telomeres in the hepatocytes of live mice (59). This study found that the motion of telomeres in liver cells of a live mouse was far more constrained than in *ex-vivo* liver cells, such as HEK293T. These findings raise an important red flag for cell culture studies: what is observed in cell culture may not reflect reality in whole mammals. Future work in live animals will be vital to resolve this issue.

Regardless of technique, a primary consideration for all single locus visualization methods is the signal-to-noise ratio (SNR). A single fluorescent molecule is often unde-

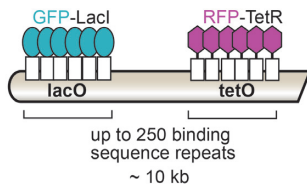
tectable over noise, and thus many fluorescent molecules should be recruited for a clear signal. This is the reason for the large size of the repressor array necessary for the LacO and TetO systems. TALEs, zinc finger proteins, and dCas9 systems originally targeted repetitive sequences to increase the number of photons detected. Newer studies have proposed multiple ways to overcome the limitation to repetitive genomic loci (Figure 1). The sgRNAs used in dCas9 systems can be modified to include RNA stem-loop sequences that recruit fluorescently tagged RNA-binding proteins (such as PP7 and MS2) (49,50,53,56,58,60,61). The latest variant of this approach is CRISPR–Sirius (50) (Figure 1C). A major advance here was the finding that stability of the modified sgRNA increased considerably when a thermostable octet of MS2 aptamers was used instead of 14 linear MS2 repeats (50). As a result, while targeting a single locus with dCas9 using a sgRNA with 14× MS2 repeats was undetectable, a smaller, thermostable 8× MS2 sgRNA efficiently labeled the locus on all homologous chromosomes. The disadvantage of CRISPR–Sirius is that it employs genetically encoded CRISPR elements and RNA binding-fluorophores. This means that CRISPR–Sirius may be difficult to use in primary cells. Wang *et al.* developed LiveFISH (26), a dCas9 based imaging technique that can efficiently be used on primary cells. This system employs dCas9 and Cy3-labeled guide RNA assembled *ex vivo* as fluorescent ribonucleoproteins (fRNPs) which can be delivered to cells by electroporation. Interestingly, the majority of the sgRNA signal was lost within 4 hours, yet the targeted repetitive locus showed rapid and long-lasting labeling with approximately 4-fold higher SNR compared to dCas9–EGFP. Importantly, the fRNPs did not accumulate in the nucleolus, a prevalent issue with dCas9–EGFP. While this approach has great promise, it has only been demonstrated to work at repetitive loci thus far.

Another means of overcoming the issue of SNR is to recruit more fluorescent dCas9 molecules to the locus of interest. Chimeric array of gRNA oligonucleotides (CARGO) uses tandemly expressed 12 sgRNAs, to recruit 12 dCas9–EGFP molecules to a genomic region spanning approximately 2kb (62) (Figure 1C). However, this requires construction of a plasmid to express the sgRNAs but does allow non-repetitive loci to be visualized. An alternative approach to CARGO is CRISPR–Tag. In this approach, a 250bp repeating sequence is integrated near the locus of interest (63) (Figure 1C). The repeating units of the integrated sequence are binding sites for four different sgRNAs. Instead of the typical dCas9–EGFP, Cas9 is tagged with 14× GFP11, a fragment of GFP when complemented with GFP1-10, forms a functional fluorescent protein (64). The disadvantage of CRISPR–Tag is that GFP1-10 must be expressed exogenously.

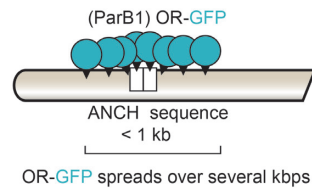
An alternative to the dCas9 based systems is the ANCHOR3/ParB DNA labeling system. In a manner like CRISPR–Tag, a short (<1 kb) sequence is integrated near the locus of interest. This sequence recruits 9 dimers of the bacterial ParB protein tagged with a fluorophore (OR–GFP) (65,66) (Figure 1A). Importantly, the ANCHOR3 system relies on the local spreading of ParB proteins around the locus of interest, which amplifies the fluorescent signal.

A Genetically encoded bacterial systems

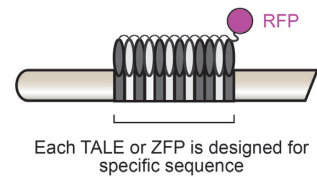
LacO / TetO systems



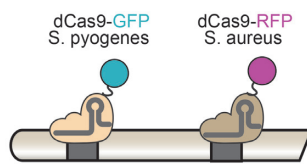
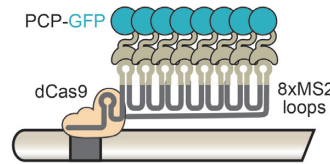
ANCHOR3 system

**B Sequence specific fluorescent proteins**

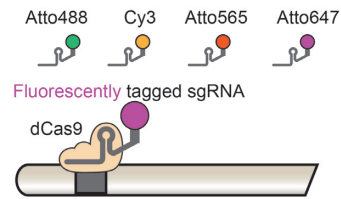
TALEs and zinc finger proteins

**C CRISPR-Cas9 based methods**

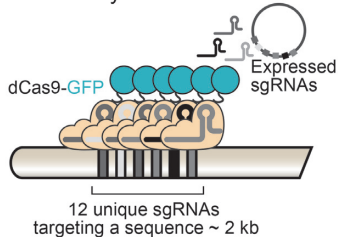
Fluorescently tagged dCas9

Extended sgRNA stem loops
(CRISPR-Sirius and others)

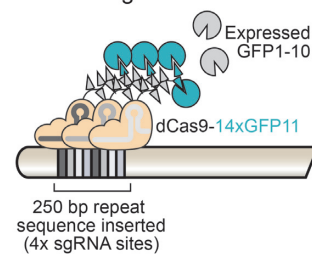
LiveFISH



CARGO system



CRISPR-Tag

**D Dynamic recruitment-based approach**

ArrayG

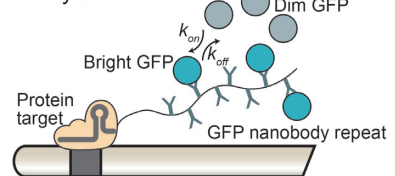


Figure 1. Systems to fluorescently label genomic loci in living cells. **(A)** The genetically encoded bacterial systems require insertion of a repeat binding sequence into the genome. This can be large, in the case of a lac or tet operator array, or small as in the case of the ANCHOR system. The repeat sequence recruits a fluorescently tagged molecule specific to the repeat. While the lacO/tetO systems require many binding sites to visualize a locus, the ANCHOR system spreads over the surrounding chromatin. **(B)** Fluorescently labeled TALEs and zinc finger proteins (ZFPs) are designed to bind to a specific locus. **(C)** CRISPR-Cas9 based methods to visualize genomic sites in living cells include the original fluorescently tagged, catalytically dead Cas9 (dCas9). Multiple sites can be uniquely visualized using Cas9 variants. To amplify the signal, the sgRNA can be modified to include multiple binding sites for fluorescently labeled RNA binding proteins. We highlight CRISPR-Sirius but there are many examples of this approach (see main text). Alternative methods to boost the signal include the CARGO system, where multiple sgRNAs with homology over a 2kb region are expressed from an exogenously supplied plasmid. CRISPR-tag has two amplification approaches, the first is the insertion of a 250 bp sequence consisting of four unique sgRNAs. The second amplification step is through tagging of dCas9 with 14 copies of GFP11. GFP11-10 is expressed exogenously. Upon complementation of GFP11 with GFP1-10, a fluorescent signal is obtained. The newest visualization method is LiveFISH. Here sgRNAs are fluorescently tagged with dye molecules. **(D)** While not yet used with Cas9 for locus-specific imaging, ArrayG may offer temporally unlimited imaging. This system takes advantage of a dim GFP that becomes brighter upon binding to a GFP nanobody. The recruitment of the dim GFP to the nanobody is dynamic, meaning that after bleaching there is a high probability of exchange with another unbleached dim GFP molecule.

Another exciting approach to overcome SNR is to change the properties of the fluorescent molecule so that when it is bound to its target, it becomes brighter. Yet to be applied for imaging of specific loci, ArrayG, ArrayD, and ArrayG/N tags exemplify this fluorogenic enhancement approach (67) (Figure 1D). Based on genetically encoded camelid nanobody tags, monomeric wild-type green fluorescent protein brightens ~26-fold when bound to the array (67). This system was employed to track H2B molecules at 0.5 Hz for over an hour generating statistically robust trajectory data enabled by an unlimited pool of dim, free binders that can be stochastically exchanged on the array where they become brighter. This system could potentially com-

plement the Janelia-Fluor Halo tags for multicolor imaging (68). Finally, these tags are smaller than alternatives such as the SunTag, Spaghetti monster, or MS2/PP7 increasing the chance of a functionally tagged protein (69–72).

Single particle tracking of chromatin

Early experiments in mammalian cells using fluorescence recovery after photobleaching (FRAP) and bulk tracking of chromatin suggested that chromatin was generally immobile (73–75). Later with the above described innovations to study single genomic loci, single particle tracking (SPT) became the most frequently used method to study chro-

matin motion (76). SPT methods must distinguish the signal of biomolecules labeled with either organic dyes or fluorescent proteins from background, to localize and track their positions over time (Figure 2A) (77–79). However, the relative thickness of the mammalian cell nucleus, its high auto-fluorescence background, and the fact that many of the key molecular species are present at high copy numbers, make single-molecule detection in the nucleus challenging. This problem is particularly pronounced when using wide-field epi-fluorescence microscopes, which excite all molecules along the illumination path, leading to higher background that can easily overwhelm the signals of individual molecules. To avoid this limitation, several systems have been employed to decrease the excitation volume outside that afforded by epi-illumination and improve signal sensitivity. These include total internal reflection fluorescence (TIRF), reflected light-sheet microscopy, lattice light sheet microscopy, highly inclined thin illumination (HILO) and fast optical sectioning techniques such as spinning disk confocal microscopy (66,78,80–88).

Monitoring global chromatin dynamics

Many techniques and methods exist to study the dynamics of single genomic loci. In the next section we will discuss the evolution and development of new techniques to study whole genome dynamics and cover the key findings from these studies. Single particle tracking photoactivated localization microscopy (sptPALM) has been previously used to study the motion of membrane proteins such as Gag and VSVG as well as AMPA receptor trafficking (77,89,90). SptPALM combines PALM with SPT using many rounds of activation, localization and bleaching of photoactivatable fluorescent-proteins. This was recently used to study single H2B molecules tagged with a photoactivatable mCherry in a variety of mammalian cells (Figure 2B) (91). Building on previous work from the same group (85), Nozaki *et al.*, found that nucleosomes form clusters called chromatin domains rather than being randomly distributed. Interestingly, treatment of cells with the histone deacetylase (HDAC) inhibitor trichostatin A (TSA) or the knockdown of cohesin both increased the motion of H2B and led to less well defined chromatin domains (91). Of note is the observation that knockdown of CTCF, which, like cohesin, is involved in formation of chromatin loops, did not affect domain size or H2B motion. This study also successfully tracked the motion of replication domains using cyanine 3-deoxycytidine triphosphate (Cy3-dCTP) and found that early replicating domains moved more than mid-late replicating domains. Dual tracking of a tagged H2B and Cy3-dCTP showed that nucleosome movement overlapped with replication domain movement. However, due to the nature of sptPALM the chance of a colocalizing H2B molecule with a Cy3-dCTP domain is low. Thus, it is difficult to build a robust argument for or against correlated motion, that is motion in the same direction, using sptPALM.

Another method to study bulk chromatin motion is displacement correlation spectroscopy (DCS) (Figure 2C) (84). Previously used to monitor the mobility of membrane proteins in living cells (92,93), DCS measures the direction and magnitude of chromatin movements simultane-

ously across the entire nucleus through time (84). While DCS presents a global view of chromatin dynamics, it does so using large interrogation windows of sub-micron size. Chromatin motion occurs at the nanoscale level and thus, it is necessary to develop techniques that allow for nanometer scale interrogation of the nucleus.

Developed to fit this need, Dense Flow reConstruction and Correlation (DFCC) allows for detection of chromatin motion at nanoscale resolution (94). DFCC utilizes Optical Flow to estimate the motion of dense fluorescently labeled chromatin by means of flow fields, thus giving access to the direction and magnitude of chromatin motion at sub-pixel resolution throughout the whole nucleus simultaneously (Figure 2D). The autocorrelation of estimated flow fields is computed and allows for coherent motion of domains to be detected and quantified. The correlation function was calculated, then fitted over space and for different time lags provides characteristic parameters of the coherently moving chromatin domains such as correlation length and the smoothness of flow fields with nano-scale resolution (94). DFCC allows for nanometer resolution of correlated motion but, it does not spatially resolve the magnitude of dynamics for a time series, from which biophysical parameters are inferred. However, DFCC can detect long-range correlated motion extending over several microns that was reduced by the inhibition of transcriptional elongation (described in detail in the following section) (94). To solve this, DFCC has been further developed into a new approach called High resolution Diffusion mapping (Hi-D) (95). Hi-D infers virtual trajectories of each pixel over time, from which information such as the Mean Square Displacement (MSD) is calculated. Bayesian inference is then used to classify the type of motion for each trajectory. Inferring the physical parameters and motion modes for each pixel avoids averaging of information from many pixels and thus provides spatially resolved motion maps of the entire nucleus (Figure 2E) (95).

With the tools and techniques described above (see Table 1 for a list of advantages and disadvantages), the path is clear to tackle several open questions related to chromatin dynamics. In the next section, we will specifically focus on recent studies probing the interplay between transcription and chromatin motion.

DYNAMICS OF CHROMATIN DURING TRANSCRIPTION

Imaging of transcription dynamics

The recent ability to monitor many stages of transcription such as mRNA turnover using optical approaches in living cells has also paved the way to study their dynamics (96,97). Using fluorescent RNA-binding proteins; fluorogenic tags or RNAs; molecular beacons or fluorescently tagged dCas13 it is now possible to visualize single RNAs in living cells (69,97–103). These studies have led to an abundance of insight on nascent transcriptional dynamics. One of the mostly intensively studied transcriptional process is ‘bursting’, where RNA molecules are not formed at a constant rate, but many RNAs are produced almost concurrently. This is then followed by a period of transcriptional inactivity. Bursting can be explained by using a two-state

Table 1. Summary of methods to study chromatin dynamics

Method	Motion information	Advantages	Disadvantages	Analysis approach	Refs
Single locus tracking	Local	Easy analysis; locus specific information; easy to design multi-color experiment for trajectory normalization.	Possibly need to engineer cell lines; only local information in trajectories, may have SNR issues.	Many tracking methods and free software including Fiji plugin Trackmate; u-Track, HybTrack and Ilastik. Movement often quantified by mean square displacement (MSD) analysis.	(6,66,76–78,120–123)
Single-nucleosome tracking-PALM	Local, Global	Robust trajectories, Single-nucleosome tracking	Difficult to track multiple colors simultaneously; short time interval that makes chromatin motion is highly heterogeneous; difficult to place in the context of global chromatin organization and its enduring configurational changes.	Single particle tracking followed by mapping of the nucleosome positions. Cluster analysis and heat maps of domain dynamics can also be obtained.	(17,77,91,124)
Displacement correlation spectroscopy (DCS)	Bulk and Global	Calculates the spatio-temporal correlation of coherent chromatin motion at micro-scale through the entire nucleus; the calculated correlation is for both direction and magnitude of flow fields ; provides smoothness parameter that quantifies the motion sharpness of transitions between chromatin domains ; no dye restrictions; can be applied to two color imaging.	Relatively large interrogation window (local chromatin motion is missing); requires fast computations, time consuming; required high SNR for better estimation of displacement vectors; no spatially resolved biophysical parameters obtained.	Particle image velocimetry followed by spatial displacement autocorrelation function over time lags.	(84)
Dense Flow reconstruction and Correlation (DFCC)	Bulk and Global	Calculates the spatio-temporal correlation (for both direction and magnitude) of coherent chromatin motion with nano-scale sensitivity over the entire nucleus; the calculated correlation is for both direction and magnitude of flow fields; provides smoothness parameter that quantifies the motion sharpness of transitions between chromatin domains; no dye restrictions; can be applied to two color imaging.	No spatially resolved biophysical parameters obtained.	DFCC spatially and temporally correlates the flow field in order to quantify the extent to which correlated motion at nanoscale. The result is a spatially averaged correlation curve which is further quantified in order to yield the correlation length and the smoothness parameter.	(94)
High resolution Diffusion mapping (Hi-D)	Bulk, local and Global	The capability to track bulk structures with sub-pixel information; any fluorescence images can be analyzed; no need for prior experiences in gene labeling, no need to use advanced microscopes; thousands of trajectories generated for the entire nucleus; a Bayesian inference to select a suitable interpretive model for MSD curve; yield conclusive and spurious-free parameter estimates within the entire nucleus simultaneously; possible to use with multi-color imaging, can be applied to two color imaging.	MSD of virtual particles (pixels of DNA labelled chromatin); OF has a smoothness constraint that prevents capturing completely random motion; high-speed computer is needed.	Hi-D connects the flow fields (by means Optical of Optical Flow) over time in order to track local motion from which the MSD can be calculated. Fitting of MSD curves with five different diffusion models using Bayesian inference defines accurately the diffusion model of each trajectory over thousands of trajectories and therefore extract the diffusion parameters, such as diffusion constant, anomalous exponent and drift velocity.	(95)

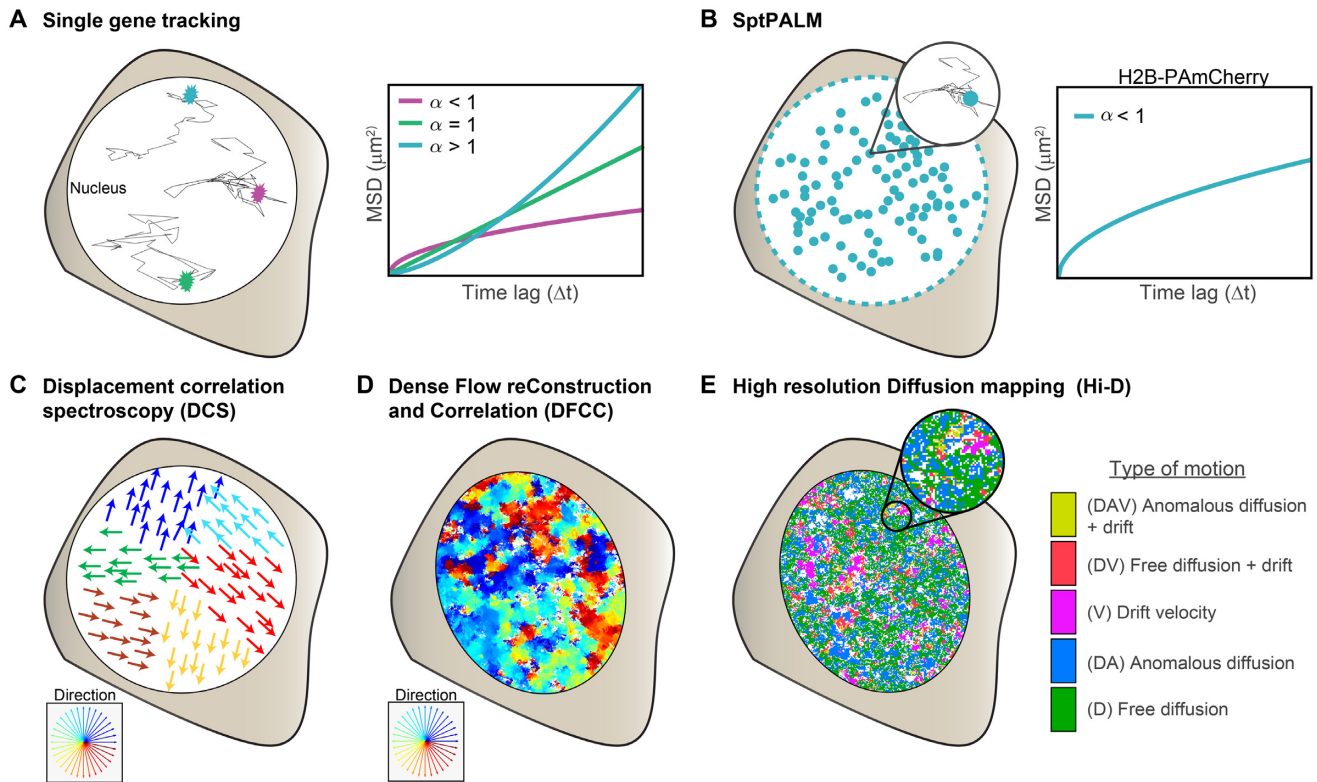


Figure 2. Live-cell chromatin imaging techniques. (A) Single genomic loci can be visualized using techniques described in Figure 1 and tracked over time. Shown are three trajectories of different motion types. MSD analysis of the trajectories is used to distinguish the motion types: anomalous/sub diffusion $\alpha < 1$, Brownian motion $\alpha = 1$ and directed $\alpha > 1$. (B) Single particle tracking photoactivated localization microscopy (SptPALM) activates a few molecules at a time. They are then tracked until bleached and this process reiterated to generate hundreds of short trajectories. The sum of the MSD for all trajectories is the calculated (C) Displacement correlation spectroscopy (DCS). Images are divided into interrogation windows (sub-micron scale), and particle image velocimetry (PIV) is used to estimate the displacement vectors. (D) Dense Flow reConstruction and Correlation (DFCC) uses optical flow to estimate the velocity vectors between pairs of images for each pixel at nanoscale precision. (E) Motion map analysis for an entire nucleus using Hi-D. The displacement vectors are estimated as in (D) and are connected over time to generate trajectories of each pixel. The MSD is calculated, followed by Bayesian analysis to determine the motion type for each trajectory. The spatial distribution of the selected models for each pixel is shown as a color map.

model with an active and inactive promoter state, each characterized by the burst size, burst frequency and burst duration parameters (1,104,105). Nascent transcription can also be studied indirectly by detecting and studying the dynamics of binding proteins such as transcription factors (TF) (106–109). Although many efforts have been made to link the kinetics of TFs to transcription bursting, their causal relationship remains unclear. The impediment is the technological barrier to measure the structure and dynamics for both the gene of interest and the transcription factor simultaneously in the same cell. This necessitates further developments in *in vivo* imaging at the single molecule level or at high spatial resolution to capture the dynamic behavior of TFs. In the following section, we focus on how chromatin dynamics change during the transcription.

Single gene dynamics during transcription

How chromatin dynamics change during transcription is largely unknown. SPT of yeast loci revealed that transcriptional elongation is not required to enhance locus movement since the inhibition of RNA Pol II had no effect on the motion of a tagged locus (110). Yet, local chromatin movement does increase when certain transcriptional activators,

such as VP16, are targeted to a chromatin locus. However, this increased motion does not require the activity of RNA polymerase, begging the question of what is responsible for this effect. Interestingly, VP16 recruits a number of factors to activate transcription including the INO80 and Swr1 chromatin remodeling complexes (111,112). While Swr1 is not required for VP16 increased chromatin motion, INO80 is (110). Thus, in budding yeast, it appears that transcription is not necessary to drive increased chromatin motion, but rather remodeling of local chromatin structure is required.

Another study used the ANCHOR3 system in combination with MS2-labeled mRNAs to study the motion of a tagged genomic locus in human cells (66). The advantage of this system over the yeast studies was the ability to measure motion before and after the appearance of a nascent mRNA as opposed to assuming that the locus was always transcriptionally active. Analysis of the motion of ANCHOR tagged loci before and after transcription activation showed that transcription initiation by RNA polymerase II correlated with increased locus confinement (66). Interestingly, the adenosine analog and transcriptional elongation inhibitor, 5,6-Dichloro-1- β -D-ribofuranosylbenzimidazol (DRB), did not seem to affect

the motion of the tagged transcribed locus. This suggests that transcription initiation induces the confinement of the locus, a hypothesis supported by the observation that the transcriptional initiation inhibitor, triptolide (TRP), when added to transcriptionally stimulated cells, releases locus confinement. While it is unclear if confining the motion of a locus plays a functional role in transcription, it may be that its confinement promotes the formation of transcriptional domains. Interestingly, Nozaki *et al.* showed that DRB treatment did not affect H2B chromatin domain size but did increase dynamics in general (91). More experiments will be required to understand the exact effect of DRB. It is likely that removal of elongation complexes by DRB could release constraint, DRB may also have other effects and more precise molecular manipulations of transcription should be performed.

Using the CARGO-dCas9 imaging system, Gu *et al.*, monitored the *Fgf5* enhancer locus in mouse embryonic stem cells (mESC) and in differentiated mouse epiblast-like cells (mEpiLC) (62). They find that locus mobility increases at the *Fgf5* enhancer locus in mEpiLCs versus mESCs and that the same effect is observed at the *Fgf5* promoter locus. Since the *Fgf5* enhancer locus is active during the mESC to mEpiLC transition they propose that transcriptional activation increases locus motion. In contrast to Nozaki *et al.*, and Germier *et al.*, these authors find that DRB, TRP as well as the transcriptional elongation inhibitor, flavopiridol, all reduce enhancer mobility (62). This is the first study to monitor locus dynamics at enhancer and promoter pairs and to monitor changes in dynamics during differentiation. To explain the increase of mobility of *cis* regulators, the authors propose a ‘stirring model’, in which the transcription induced motion affords a non-thermal molecular agitation that can ‘stir’ chromatin domains. Based on this model, the contact frequencies of enhancer-promoter may increase due to the stochastic confrontations within the topologically associating domain (TAD), not as a result of the establishment of stable enhancer-promoter loops (113).

A more recent study combined genome editing tools and triple-color live cell imaging to correlate changes of enhancer/promoter morphology, dynamics and genome activity (114). In *Drosophila* embryos, the authors use the ANCHOR system to monitor the location of the endogenous *eve* gene, MS2 stem loops integrated at the endogenous *eve* gene, and PP7 stem loops at an integrated *eve* reporter. The nascent transcripts were visualized by maternal expression of the corresponding fluorescent stem loop binding proteins. The physical distance between tagged promoter and enhancer was measured in order to report topological changes at the single cell level during different transcriptional stages. The authors find that sustained physical proximity is necessary for continuous transcription initiation and suggest that confined transcription may stabilize the paired loci. Importantly, the authors could show that competition between two promoters can in fact cause developmental defects (114). While, this study does not resolve the question of whether chromatin topology changes first to drive transcription or vice versa, it does show that the proximity of feedback loops is required to start transcription with associated changes in chromatin topology driving more transcription.

Genome-wide chromatin dynamics and organization during transcription

While monitoring single genes during transcription provide local information, studying whole genome dynamics may prove to be a more fruitful approach to understand how transcription changes chromatin organization. In one study, DFCC was used to monitor if correlated motion changes during transcriptional perturbation (94). The authors found that in transcriptionally active cells, the motion of chromatin domains exhibits long-range coherence, which is lost by halting transcription initiation with DRB. In addition to the correlation length, the magnitude of motion was decreased in these conditions. In contrast, correlation length and magnitude of motion was largely unaffected by inhibition of transcription elongation by TPL. Interestingly, the boundary between neighboring domains was far sharper for actively transcribing cells and smoother for inactive cells. In a new study, structure illumination microscopy (SIM) was used to improve the spatial resolution of chromatin imaging (42). The enhanced spatial resolution using SIM resolved the oscillation change in correlation length of 0.5 μm between adjacent, coherently moving domains. This suggests visco-elastic coupling of domain movement that can be likened to chromatin ‘breathing’ (42). The mechanical and biophysical characterization of chromatin observed in this study are consistent with a model of coherent motion of highly-viscous droplet-like domains (42,94,115).

Single nucleosome imaging of tagged histones over the nucleus was applied to study the dynamics and organization of chromatin during transcription in living human cells (116). This study took advantage of the combination of super resolution photoactivated localization microscopy and SPT to have a spatial resolution at the nucleosome level (91). Chromatin mobility was investigated under different transcriptional states, by using active and inhibited RNA polymerase II (RNA Pol II). Interestingly, the authors found that active RNA Pol II constrains the global motions of chromatin domains, while the movement of chromatin increased when RNA Pol II was inactivated. Moreover, trapping U2OS cells in G0 by serum starvation, as an indication for reduced RNA Pol II production, led to an increase in chromatin mobility. These findings suggested that active RNA Pol II clusters form chromatin domain looping networks for several intra- and inter-chromosomal contacts (116). Using Hi-D, the motion types of both chromatin and RNA Pol II during transcription were categorized for the entire nucleus. This classification resolved motion-based domains spatially partitioned into 0.3–3 μm in a mosaic-like shape, which is disengaged from chromatin compaction (95). This domain like pattern was altered in response to transcriptional activity. In contrast to chromatin dynamics, RNA Pol II dynamics are decreased in actively transcribing cells, compared to the inactive transcribed state (95). These results reinforce the supposition that chromatin dynamics are dictated by interchromatin contacts (95,116). Also, suggesting that transcription complex (TFs and RNA Pol II) can act as hub that temporarily connects active DNA regions, and therefore, limiting chromatin motion (95,116,117).

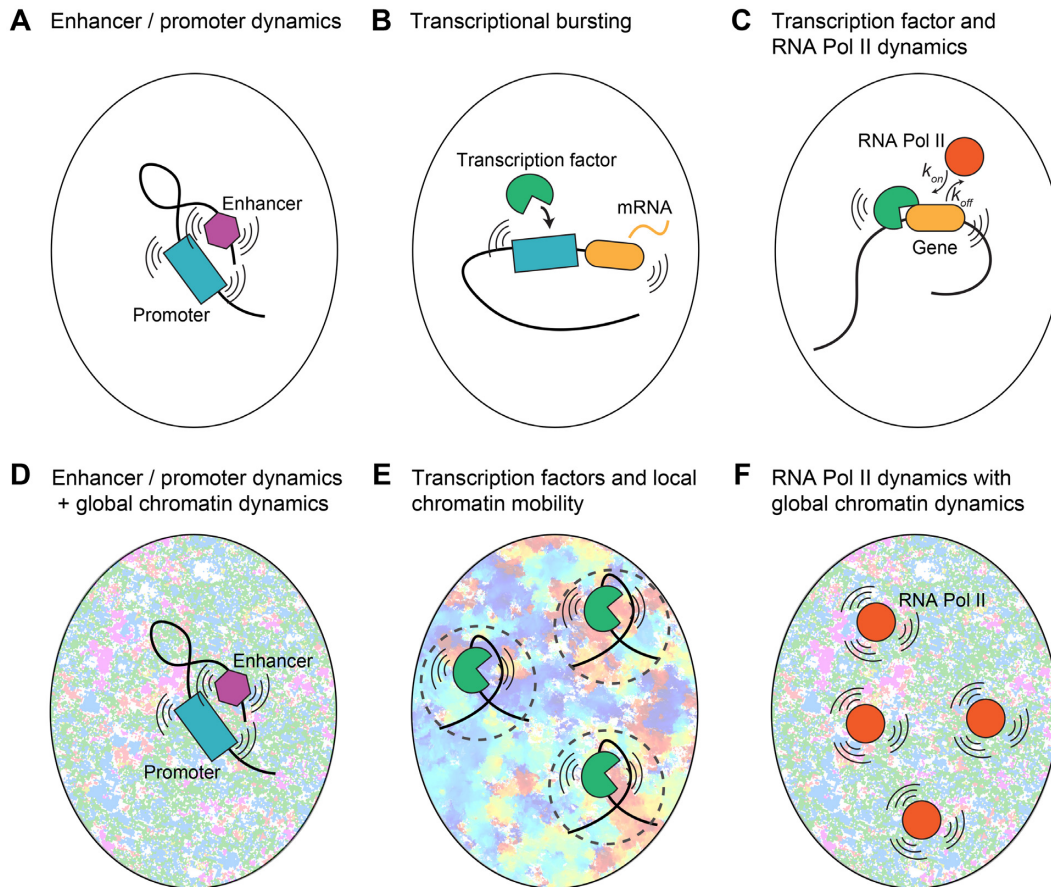


Figure 3. Open questions regarding spatio-temporal genome organization during transcription. The techniques described in this review can address many open questions on chromatin organization, dynamics and transcription. A few of these are described here: **(A)** Live-cell, two-color imaging of enhancers and promoter interaction will be important to understand the spatial and temporal constraints of transcriptional regulation by enhancers. For example, do enhancers need to ‘touch’ promoters to engage transcription or simply move into the near vicinity? **(B)** How is transcriptional bursting regulated by transcription factors? This could be addressed using multi-color imaging of fluorescently tagged transcription factors, labeled mRNAs and labeled genomic loci. **(C)** What is the relationship between transcription factor and RNA Pol II dynamics? It will be necessary to use three-color single molecule imaging of genomic loci, fluorescently labeled RNA Pol II and transcription factors. Long acquisitions will be necessary for robust data. Answering this may be facilitated using organic fluorophores or the ArrayG technology, described in this review, coupled with lattice light sheet microscopy. **(D)** How do enhancer promoter dynamics affect global chromatin dynamics? Coupling techniques like Hi-D, which can visualize whole genome dynamics, with multicolor imaging of single tagged genomic loci will show how loci can ‘move through’ chromatin. **(E, F)** Similarly to **(D)**, fluorescently tagged transcription factors or RNA Pol II coupled with Hi-D or DFCC can address how transcription factors affect surrounding chromatin dynamics and structure.

Taken together these studies suggest that chromatin configuration changes during transcription initiation. This conclusion is supported by perturbation experiments in which transcription is halted using DRB. Treatment with DRB for a short period of time (a few minutes) induces a small re-configuration of promoters, disturbs the assembly process of the preinitiation complex and, most importantly, disrupts RNA Pol II recruitment (66,94,118,119). In contrast, cell incubation with DRB for hours as well as serum starvation, are likely to disassemble the preinitiation complex (PIC) and may therefore increase chromatin mobility associated with PIC collapse. Contrariwise, reduction of chromatin mobility without drug treatment or serum starvation, proposes that PIC assembles around the DNA and inhibits chromatin motion by anchoring adjacent chromatin fibers, beside of its vital role in transcription initiation (66,95,116).

CONCLUSION AND OUTLOOK

Advances in gene editing, and live cell imaging techniques have greatly improved our understanding of molecular mechanisms regulating gene expression in time and space. In this review, we have painted in broad strokes, a few key concepts derived from these recent studies regarding genome organization, chromatin dynamics, and gene expression. All together, these studies highlight the decidedly dynamic yet regulated motion of chromatin during transcription. Live cell studies bolster the evidence that topological assemblies can shape chromatin inside the nucleus to achieve transcription initiation and potentially other gene-regulatory activities. Based on the information provided in these studies, we suggest an enhancer-mediated regulatory mechanism commanded by dynamic protein–DNA and protein–protein interactions for transcription initiation

(Figure 3A). While much is already known concerning transcriptional bursting, the techniques described in this review will be essential to understand how transcription factors modulate various bursting characteristics (Figure 3B).

Finally, to understand the regulatory mechanisms of the transcriptional machinery, more studies will be essential to elucidate how RNA Pol II and transcription factors modulate chromatin dynamics and whether this motion is a cause or consequence of transcription (Figure 3C, F). One way to test cause or consequence is by ‘gain of function’ or ‘separation of function’ experiments. As described above, Neumann *et al.*, targeted transcriptional activators to genomic loci in budding yeast and measured their mobility as well as their transcriptional output (110). Using this approach, the authors showed that targeting one transcriptional activator (VP16) increased chromatin mobility while another did not (Gal4 domain) and concluded that transcriptional activity does not drive chromatin movement in yeast but was rather a result of chromatin remodeling. The same approach could be used in mammalian cells: target a transcriptional activator to a specific genomic locus and then measure its mobility. This experiment would be even more powerful if coupled with a live cell imaging readout for transcriptional activity such as that used in Germier *et al.* An alternative approach to probe whether mobility is a cause or consequence of transcription would be to change locus mobility, through chromatin remodeling enzyme targeting (110), and measure transcriptional output. Ultimately, this is a difficult question to answer due to the inter-related outcomes of chromatin remodeling and transcription and would require sampling of many genomic loci. However, the tools are at hand to test this hypothesis and many others. These advances will be driven by new live cell imaging techniques at the single cell and nanoscale levels. In addition, development of single molecule imaging strategies and probes will allow in-depth observation of TF and RNA Pol II interactions during all transcription stages. The combination of single gene and global chromatin analysis at high spatial and temporal resolutions is importantly needed to simultaneously analyze the interplay between structural and dynamic aspects of chromatin experimentally at both local and global scales (Figure 3D-F). Furthermore, the coupling between single cell sequencing methods, polymer modeling and live cell imaging will permit a complete view of genome organization in space and time.

ACKNOWLEDGEMENTS

This work was supported by the Office of the Provost, Faculty of Arts & Sciences and Center for Advanced Imaging at Harvard University. This review is dedicated to the memory of Michael H. Hauer, an amazing scientist and friend.

FUNDING

Funding for open access charge: Center for Advanced Imaging at Harvard University.

Conflict of interest statement. None declared.

REFERENCES

- Brouwer, I. and Lenstra, T.L. (2019) Visualizing transcription: key to understanding gene expression dynamics. *Curr. Opin. Chem. Biol.*, **51**, 122–129.
- Tsukamoto, T., Hashiguchi, N., Janicki, S.M., Tumber, T., Belmont, A.S. and Spector, D.L. (2000) Visualization of gene activity in living cells. *Nat. Cell Biol.*, **2**, 871–878.
- Nagai, L.A.E., Park, S.J. and Nakai, K. (2019) Analyzing the 3D chromatin organization coordinating with gene expression regulation in B-cell lymphoma. *BMC Med. Genomics*, **11**, 19–29.
- Symeonidou, I.E., Taraviras, S. and Lygerou, Z. (2012) Control over DNA replication in time and space. *FEBS Lett.*, **586**, 2803–2812.
- Scalfani, R.A. and Holzen, T.M. (2007) Cell cycle regulation of DNA replication. *Annu. Rev. Genet.*, **41**, 237–280.
- Seeber, A., Hauer, M.H. and Gasser, S.M. (2018) Chromosome dynamics in response to DNA damage. *Annu. Rev. Genet.*, **52**, 295–319.
- Seeber, A. and Gasser, S.M. (2017) Chromatin organization and dynamics in double-strand break repair. *Curr. Opin. Genet. Dev.*, **43**, 9–16.
- Meldi, L. and Brickner, J.H. (2011) Compartmentalization of the nucleus. *Trends Cell Biol.*, **21**, 701–708.
- Cremer, C.T., Cremer, T. and Cremer, C. (2016) Chromosome territories, nuclear architecture and gene regulation in mammalian cells. *Nat. Rev. Genet.*, **2**, 292–301.
- Florescu, A.M., Therizols, P. and Rosa, A. (2016) Large scale chromosome folding is stable against local changes in chromatin structure. *PLoS Comput. Biol.*, **12**, e1004987.
- Amitai, A., Seeber, A., Gasser, S.M. and Holcman, D. (2017) Visualization of chromatin decompaction and break site extrusion as predicted by statistical polymer modeling of single-locus trajectories. *Cell Rep.*, **18**, 1200–1214.
- Miné-Hattab, J., Recamier, V., Izeddin, I., Rothstein, R. and Darzacq, X. (2017) Multi-scale tracking reveals scale-dependent chromatin dynamics after DNA damage. *Mol. Biol. Cell*, **28**, 3323–3332.
- Dixon, J.R., Selvaraj, S., Yue, F., Kim, A., Li, Y., Shen, Y., Hu, M., Liu, J.S. and Ren, B. (2012) Topological domains in mammalian genomes identified by analysis of chromatin interactions. *Nature*, **485**, 376–380.
- Kalhor, R., Tjong, H., Jayathilaka, N., Alber, F. and Chen, L. (2012) Genome architectures revealed by tethered chromosome conformation capture and population-based modeling. *Nat. Biotechnol.*, **30**, 90–98.
- Sexton, T., Yaffe, E., Kenigsberg, E., Bantignies, F., Leblanc, B., Hoichman, M., Parrinello, H., Tanay, A. and Cavalli, G. (2012) Three-dimensional folding and functional organization principles of the *Drosophila* genome. *Cell*, **148**, 458–472.
- Entrevan, M., Schuettengruber, B. and Cavalli, G. (2016) Regulation of genome architecture and function by polycomb proteins. *Trends Cell Biol.*, **26**, 511–525.
- Hihara, S., Pack, C.G., Kaizu, K., Tani, T., Hanafusa, T., Nozaki, T., Takemoto, S., Yoshimi, T., Yokota, H., Imamoto, N. *et al.* (2012) Local nucleosome dynamics facilitate chromatin accessibility in living mammalian cells. *Cell Rep.*, **2**, 1645–1656.
- Deplancke, B., Alpern, D. and Gardeux, V. (2016) The genetics of transcription factor DNA binding variation. *Cell*, **166**, 538–554.
- Hansen, A.S., Pustova, I., Cattoglio, C., Tjian, R. and Darzacq, X. (2017) CTCF and cohesin regulate chromatin loop stability with distinct dynamics. *Elife*, **6**, e25776.
- Hansen, A.S., Amitai, A., Cattoglio, C., Tjian, R. and Darzacq, X. (2020) Guided nuclear exploration increases CTCF target search efficiency. *Nat. Chem. Biol.*, **16**, 257–266.
- Fudenberg, G., Imakaev, M., Lu, C., Goloborodko, A., Abdennur, N. and Mirny, L.A. (2016) Formation of chromosomal domains by loop extrusion. *Cell Rep.*, **15**, 2038–2049.
- Nuebler, J., Fudenberg, G., Imakaev, M., Abdennur, N. and Mirny, L.A. (2018) Chromatin organization by an interplay of loop extrusion and compartmental segregation. *Proc. Natl. Acad. Sci. U.S.A.*, **115**, E6697–E6706.
- Rao, S.S.P., Huang, S.C., Glenn St Hilaire, B., Engreitz, J.M., Perez, E.M., Kieffer-Kwon, K.R., Sanborn, A.L., Johnstone, S.E.,

- Bascom, G.D., Bochkov, I.D. *et al.* (2017) Cohesin loss eliminates all loop domains. *Cell*, **171**, 305–320.
24. Sanborn, A.L., Rao, S.S.P., Huang, S.-C., Durand, N.C., Huntley, M.H., Jewett, A.I., Bochkov, I.D., Chinnappan, D., Cutkosky, A., Li, J. *et al.* (2015) Chromatin extrusion explains key features of loop and domain formation in wild-type and engineered genomes. *Proc. Natl. Acad. Sci. U.S.A.*, **112**, E6456–E6465.
 25. Hauer, M.H., Seeber, A., Singh, V., Thierry, R., Sack, R., Amitai, A., Kryzhanovska, M., Eglinger, J., Holcman, D., Owen-Hughes, T. *et al.* (2017) Histone degradation in response to DNA damage enhances chromatin dynamics and recombination rates. *Nat. Struct. Mol. Biol.*, **24**, 99–107.
 26. Wang, H., Nakamura, M., Abbott, T.R., Zhao, D., Luo, K., Yu, C., Nguyen, C.M., Lo, A., Daley, T.P., La Russa, M. *et al.* (2019) CRISPR-mediated live imaging of genome editing and transcription. *Science* (80-), **365**, 1301–1305.
 27. Zhang, H., Petrie, M. V., He, Y., Peace, J.M., Chiolo, I.E. and Aparicio, O.M. (2019) Dynamic relocalization of replication origins by Fkh1 requires execution of DDK function and Cdc45 loading at origins. *Elife*, **8**, e45512.
 28. Dekker, J., Rippe, K., Dekker, M. and Kleckner, N. (2002) Capturing chromosome conformation. *Science*, **295**, 1306–1311.
 29. Dekker, J. (2006) The three ‘C’s of chromosome conformation capture: Controls, controls, controls. *Nat. Methods*, **3**, 17–21.
 30. Simonis, M., Klous, P., Splinter, E., Moshkin, Y., Willemsen, R., de Wit, E., van Steensel, B. and de Laat, W. (2006) Nuclear organization of active and inactive chromatin domains uncovered by chromosome conformation capture-on-chip (4C). *Nat. Genet.*, **38**, 1348–1354.
 31. Lieberman-aiden, E., Berkman, N.L., Van, Williams, L., Imakaev, M., Ragoczy, T., Telling, A., Amit, I., Lajoie, B.R., Sabo, P.J., Dorschner, M.O. *et al.* (2009) Comprehensive mapping of long-range interactions reveals folding principles of the human genome. *Science*, **326**, 289–293.
 32. Nagano, T., Lubling, Y., Stevens, T.J., Schoenfelder, S., Yaffe, E., Dean, W., Laue, E.D., Tanay, A. and Fraser, P. (2013) Single-cell Hi-C reveals cell-to-cell variability in chromosome structure. *Nature*, **502**, 59–64.
 33. Schwartzman, O. and Tanay, A. (2015) Single-cell epigenomics: Techniques and emerging applications. *Nat. Rev. Genet.*, **16**, 716–726.
 34. Finn, E.H., Pegoraro, G., Brandão, H.B., Valton, A.L., Oomen, M.E., Dekker, J., Mirny, L. and Misteli, T. (2019) Extensive heterogeneity and intrinsic variation in spatial genome organization. *Cell*, **176**, 1502–1515.
 35. Bintu, B., Mateo, L.J., Su, J.H., Sinnott-Armstrong, N.A., Parker, M., Kinrot, S., Yamaya, K., Boettiger, A.N. and Zhuang, X. (2018) Super-resolution chromatin tracing reveals domains and cooperative interactions in single cells. *Science*, **362**, eaau1783.
 36. Wang, S., Su, J.H., Beliveau, B.J., Bintu, B., Moffitt, J.R., Wu, C.T. and Zhuang, X. (2016) Spatial organization of chromatin domains and compartments in single chromosomes. *Science*, **353**, 598–602.
 37. Beliveau, B.J., Boettiger, A.N., Nir, G., Bintu, B., Yin, P., Zhuang, X. and Wu, C. ting (2017) In situ super-resolution imaging of genomic DNA with oligoSTORM and oligoDNA-PAINT. *Methods Mol. Biol.*, **1663**, 231–252.
 38. Beliveau, B.J., Boettiger, A.N., Avendaño, M.S., Jungmann, R., McCole, R.B., Joyce, E.F., Kim-Kiselak, C., Bantignies, F., Fonseca, C.Y., Erceg, J. *et al.* (2015) Single-molecule super-resolution imaging of chromosomes and in situ haplotype visualization using Oligopaint FISH probes. *Nat. Commun.*, **6**, 7147.
 39. Nagano, T., Lubling, Y., Várnai, C., Dudley, C., Leung, W., Baran, Y., Cohen, Mendelson, Wingett, N., Fraser, S. and Tanay, A. (2017) Cell-cycle dynamics of chromosomal organization at single-cell resolution. *Nature*, **547**, 61–67.
 40. Flyamer, I.M., Gassler, J., Imakaev, M., Brandão, H.B., Ulianov, S. V., Abdennur, N., Razin, S. V., Mirny, L.A. and Tachibana-Konwalski, K. (2017) Single-nucleus Hi-C reveals unique chromatin reorganization at oocyte-to-zygote transition. *Nature*, **544**, 110–114.
 41. Stevens, T.J., Lando, D., Basu, S., Liam, P., Cao, Y., Lee, S.F., Leeb, M., Wohlfahrt, K.J., Boucher, W., Shaughnessy-kirwan, A.O. *et al.* (2017) 3D structures of individual mammalian genomes studied by single-cell Hi-C. *Nat. Publ. Gr.*, **544**, 59–64.
 42. Miron, E., Oldenkamp, R., Pinto, D.M.S., Brown, J.M., Faria, A.R., Shaban, H.A., Rhodes, J.D.P., Innocent, C., Ornellas, S. de, Buckle, V. *et al.* (2019) Chromatin arranges in filaments of blobs with nanoscale functional zonation. bioRxiv doi: <https://doi.org/10.1101/566638>, 04 March, 2019, preprint: not peer reviewed.
 43. Barth, R., Bystricky, K. and Shaban, H.A. (2019) Coupling chromatin structure and dynamics by live super-resolution imaging. bioRxiv doi: <https://doi.org/10.1101/777482>, 20 September 2019, preprint: not peer reviewed.
 44. Robinett, C.C., Straight, A., Li, G., Wilhelm, C., Sudlow, G., Murray, A. and Belmont, A.S. (1996) In vivo localization of DNA sequences and visualization of large-scale chromatin organization using lac operator/repressor recognition. *J. Cell Biol.*, **135**, 1685–1700.
 45. Marshall, W.F., Straight, A., Marko, J.F., Swedlow, J., Dernburg, A., Belmont, A., Murray, A.W., Agard, D.A. and Sedat, J.W. (1997) Interphase chromosomes undergo constrained diffusional motion in living cells. *Curr. Biol.*, **7**, 930–939.
 46. Michaelis, C., Ciosk, R. and Nasmyth, K. (1997) Cohesins: Chromosomal proteins that prevent premature separation of sister chromatids. *Cell*, **91**, 35–45.
 47. Anton, T., Bultmann, S., Leonhardt, H. and Markaki, Y. (2014) Visualization of specific DNA sequences in living mouse embryonic stem cells with a programmable fluorescent CRISPR/Cas system. *Nucleus*, **5**, 163–172.
 48. Jinek, M., Chylinski, K., Fonfara, I., Hauer, M., Doudna, J.A. and Charpentier, E. (2012) A programmable dual-RNA-guided DNA endonuclease in adaptive bacterial immunity. *Science*, **337**, 816–821.
 49. Wang, S., Su, J.H., Zhang, F. and Zhuang, X. (2016) An RNA-aptamer-based two-color CRISPR labeling system. *Sci. Rep.*, **6**, 26857.
 50. Ma, H., Tu, L.C., Naseri, A., Chung, Y.C., Grunwald, D., Zhang, S. and Pederson, T. (2018) CRISPR-Sirius: RNA scaffolds for signal amplification in genome imaging. *Nat. Methods*, **15**, 938–931.
 51. Chen, B., Gilbert, L.A., Cimini, B.A., Schnitzbauer, J., Zhang, W., Li, G.W., Park, J., Blackburn, E.H., Weissman, J.S., Qi, L.S. *et al.* (2013) Dynamic imaging of genomic loci in living human cells by an optimized CRISPR/Cas system. *Cell*, **155**, 1479–1491.
 52. Chen, B., Hu, J., Almeida, R., Liu, H., Balakrishnan, S., Covill-Cooke, C., Lim, W.A. and Huang, B. (2016) Expanding the CRISPR imaging toolset with *Staphylococcus aureus* Cas9 for simultaneous imaging of multiple genomic loci. *Nucleic Acids Res.*, **44**, e75.
 53. Fu, Y., Rocha, P.P., Luo, V.M., Raviram, R., Deng, Y., Mazzoni, E.O. and Skok, J.A. (2016) CRISPR-dCas9 and sgRNA scaffolds enable dual-colour live imaging of satellite sequences and repeat-enriched individual loci. *Nat. Commun.*, **7**, 11707.
 54. Knight, S.C., Xie, L., Deng, W., Guglielmi, B., Witkowsky, L.B., Bosanac, L., Zhang, E.T., Beheiry, M.E., Masson, J.B., Dahan, M. *et al.* (2015) Dynamics of CRISPR-Cas9 genome interrogation in living cells. *Science*, **350**, 823–826.
 55. Ma, H., Naseri, A., Reyes-Gutierrez, P., Wolfe, S.A., Zhang, S. and Pederson, T. (2015) Multicolor CRISPR labeling of chromosomal loci in human cells. *Proc. Natl. Acad. Sci. U.S.A.*, **112**, 3002–3007.
 56. Ma, H., Tu, L.C., Naseri, A., Huisman, M., Zhang, S., Grunwald, D. and Pederson, T. (2016) Multiplexed labeling of genomic loci with dCas9 and engineered sgRNAs using CRISPRainbow. *Nat. Biotechnol.*, **34**, 528–530.
 57. Ma, H., Tu, L.C., Naseri, A., Huisman, M., Zhang, S., Grunwald, D. and Pederson, T. (2016) CRISPR-Cas9 nuclear dynamics and target recognition in living cells. *J. Cell Biol.*, **214**, 529–537.
 58. Shao, S., Zhang, W., Hu, H., Xue, B., Qin, J., Sun, C., Sun, Y., Wei, W. and Sun, Y. (2016) Long-term dual-color tracking of genomic loci by modified sgRNAs of the CRISPR/Cas9 system. *Nucleic Acids Res.*, **44**, e86.
 59. Duan, J., Lu, G., Hong, Y., Hu, Q., Mai, X., Guo, J., Si, X., Wang, F. and Zhang, Y. (2018) Live imaging and tracking of genome regions in CRISPR/dCas9 knock-in mice. *Genome Biol.*, **19**, 192.
 60. Maass, P.G., Barutcu, A.R., Shechner, D.M., Weiner, C.L., Melé, M. and Rinn, J.L. (2018) Spatiotemporal allele organization by allele-specific CRISPR live-cell imaging (SNP-CLING). *Nat. Struct. Mol. Biol.*, **25**, 176–184.
 61. Qin, P., Parlak, M., Kuscü, C., Bandaria, J., Mir, M., Szlachta, K., Singh, R., Darzacq, X., Yildiz, A. and Adli, M. (2017) Live cell imaging of low- and non-repetitive chromosome loci using CRISPR-Cas9. *Nat. Commun.*, **8**, 14725.

62. Gu, B., Swigut, T., Spencley, A., Bauer, M.R., Chung, M., Meyer, T. and Wysocka, J. (2018) Transcription-coupled changes in nuclear mobility of mammalian cis-regulatory elements. *Science*, **359**, 1050–1055.
63. Chen, B., Zou, W., Xu, H., Liang, Y. and Huang, B. (2018) Efficient labeling and imaging of protein-coding genes in living cells using CRISPR-Tag. *Nat. Commun.*, **9**, 5065.
64. Kamiyama, D., Sekine, S., Barsi-Rhyne, B., Hu, J., Chen, B., Gilbert, L.A., Ishikawa, H., Leonetti, M.D., Marshall, W.F., Weissman, J.S. *et al.* (2016) Versatile protein tagging in cells with split fluorescent protein. *Nat. Commun.*, **7**, 11046.
65. Saad, H., Gallardo, F., Dalvai, M., Tanguy-le-Gac, N., Lane, D. and Bystricky, K. (2014) DNA dynamics during early double-strand break processing revealed by non-intrusive imaging of living cells. *PLoS Genet.*, **10**, e1004187.
66. Germier, T., Kocanova, S., Walther, N., Bancaud, A., Shaban, H.A., Sellou, H., Politi, A.Z., Ellenberg, J., Gallardo, F. and Bystricky, K. (2017) Real-time imaging of a single gene reveals transcription-initiated local confinement. *Biophys. J.*, **113**, 1383–1394.
67. Ghosh, R.P., Franklin, J.M., Draper, W.E., Shi, Q., Beltran, B., Spakowitz, A.J. and Liphardt, J.T. (2019) A fluorogenic array for temporally unlimited single-molecule tracking. *Nat. Chem. Biol.*, **15**, 401–409.
68. Grimm, J.B., Muthusamy, A.K., Liang, Y., Brown, T.A., Lemon, W.C., Patel, R., Lu, R., Macklin, J.J., Keller, P.J., Ji, N. *et al.* (2017) A general method to fine-tune fluorophores for live-cell and in vivo imaging. *Nat. Methods*, **14**, 987–994.
69. Tanenbaum, M.E., Gilbert, L.A., Qi, L.S., Weissman, J.S. and Vale, R.D. (2014) A protein-tagging system for signal amplification in gene expression and fluorescence imaging. *Cell*, **159**, 635–646.
70. Viswanathan, S., Williams, M.E., Bloss, E.B., Stasevich, T.J., Speer, C.M., Nern, A., Pfeiffer, B.D., Hooks, B.M., Li, W.P., English, B.P. *et al.* (2015) High-performance probes for light and electron microscopy. *Nat. Methods*, **12**, 568–576.
71. Hocine, S., Raymond, P., Zenklusen, D., Chao, J.A. and Singer, R.H. (2013) Single-molecule analysis of gene expression using two-color RNA labeling in live yeast. *Nat. Methods*, **10**, 119–121.
72. Bertrand, E., Chartrand, P., Schaefer, M., Shenoy, S.M., Singer, R.H. and Long, R.M. (1998) Localization of ASH1 mRNA particles in living yeast. *Mol. Cell*, **2**, 437–445.
73. Abney, J.R., Cutler, B., Fillbach, M.L., Axelrod, D. and Scalettar, B.A. (1997) Chromatin dynamics in interphase nuclei and its implications for nuclear structure. *J. Cell Biol.*, **137**, 1459–1468.
74. De Boni, U. and Mintz, A.H. (1986) Curvilinear, three-dimensional motion of chromatin domains and nucleoli in neuronal interphase nuclei. *Science*, **234**, 863–866.
75. Parvinen, M. and Söderström, K.O. (1976) Chromosome rotation and formation of synapsis. *Nature*, **260**, 534–535.
76. Shukron, O., Seiber, A., Amitai, A. and Holcman, D. (2019) Advances using single-particle trajectories to reconstruct chromatin organization and dynamics. *Trends Genet.*, **35**, 685–705.
77. Manley, S., Gillette, J.M., Patterson, G.H., Shroff, H., Hess, H.F., Betzig, E. and Lippincott-Schwartz, J. (2008) High-density mapping of single-molecule trajectories with photoactivated localization microscopy. *Nat. Methods*, **5**, 155–157.
78. Gebhardt, J.C.M., Suter, D.M., Roy, R., Zhao, Z.W., Chapman, A.R., Basu, S., Maniatis, T. and Xie, X.S. (2013) Single-molecule imaging of transcription factor binding to DNA in live mammalian cells. *Nat. Methods*, **10**, 421–426.
79. Li, N., Zhao, R., Sun, Y., Ye, Z., He, K. and Fang, X. (2017) Single-molecule imaging and tracking of molecular dynamics in living cells. *Natl. Sci. Rev.*, **4**, 739–760.
80. Shechtman, Y., Gustavsson, A.-K., Petrov, P.N., Dultz, E., Lee, M.Y., Weis, K. and Moerner, W.E. (2017) Observation of live chromatin dynamics in cells via 3D localization microscopy using Tetrapod point spread functions. *Biomed. Opt. Express*, **8**, 5735.
81. Chen, B.C., Legant, W.R., Wang, K., Shao, L., Milkie, D.E., Davidson, M.W., Janetopoulos, C., Wu, X.S., Hammer, J.A., Liu, Z. *et al.* (2014) Lattice light-sheet microscopy: Imaging molecules to embryos at high spatiotemporal resolution. *Science*, **346**, 1257998.
82. Tokunaga, M., Imamoto, N. and Sakata-Sogawa, K. (2008) Highly inclined thin illumination enables clear single-molecule imaging in cells. *Nat. Methods*, **5**, 159–161.
83. Chubb, J.R., Boyle, S., Perry, P. and Bickmore, W.A. (2002) Chromatin motion is constrained by association with nuclear compartments in human cells. *Curr. Biol.*, **12**, 439–445.
84. Zidovska, A., Weitz, D.A. and Mitchison, T.J. (2013) Micron-scale coherence in interphase chromatin dynamics. *Proc. Natl. Acad. Sci. U.S.A.*, **110**, 15555–15560.
85. Shinkai, S., Nozaki, T., Maeshima, K. and Togashi, Y. (2016) Dynamic nucleosome movement provides structural information of topological chromatin domains in living human cells. *PLoS Comput. Biol.*, **12**, e1005136.
86. Chuang, C.H., Carpenter, A.E., Fuchsova, B., Johnson, T., de Lanerolle, P. and Belmont, A.S. (2006) Long-range directional movement of an interphase chromosome site. *Curr. Biol.*, **16**, 825–831.
87. Levi, V., Ruan, Q., Plutz, M., Belmont, A.S. and Gratton, E. (2005) Chromatin dynamics in interphase cells revealed by tracking in a two-photon excitation microscope. *Biophys. J.*, **89**, 4275–4285.
88. Liu, Z., Legant, W.R., Chen, B.C., Li, L., Grimm, J.B., Lavis, L.D., Betzig, E. and Tjian, R. (2014) 3D imaging of Sox2 enhancer clusters in embryonic stem cells. *Elife*, **3**, e04236.
89. Hoze, N., Nair, D., Hosy, E., Sieben, C., Manley, S., Herrmann, A., Sibarita, J.B., Choquet, D. and Holcman, D. (2012) Heterogeneity of AMPA receptor trafficking and molecular interactions revealed by superresolution analysis of live cell imaging. *Proc. Natl. Acad. Sci. U.S.A.*, **109**, 17052–17057.
90. Holcman, D., Hoze, N. and Schuss, Z. (2015) Analysis and interpretation of superresolution single-particle trajectories. *Biophys. J.*, **109**, 1761–1771.
91. Nozaki, T., Imai, R., Tanbo, M., Nagashima, R., Tamura, S., Tani, T., Joti, Y., Tomita, M., Hibino, K., Kanemaki, M.T. *et al.* (2017) Dynamic organization of chromatin domains revealed by super-resolution live-cell imaging. *Mol. Cell*, **67**, 282–293.
92. Hebert, B., Costantino, S. and Wiseman, P.W. (2005) Spatiotemporal image correlation spectroscopy (STICS) theory, verification, and application to protein velocity mapping in living CHO cells. *Biophys. J.*, **88**, 3601–3614.
93. Di Rienzo, C., Gratton, E., Beltram, F. and Cardarelli, F. (2013) Fast spatiotemporal correlation spectroscopy to determine protein lateral diffusion laws in live cell membranes. *Proc. Natl. Acad. Sci. U.S.A.*, **110**, 12307–12312.
94. Shaban, H.A., Barth, R. and Bystricky, K. (2018) Formation of correlated chromatin domains at nanoscale dynamic resolution during transcription. *Nucleic Acids Res.*, **46**, e77.
95. Shaban, H.A., Barth, R. and Bystricky, K. (2020) Nanoscale mapping of DNA dynamics in live human cells. bioRxiv doi: <https://doi.org/10.1101/405969>, 05 January 2019, preprint: not peer reviewed.
96. Horvathova, I., Voigt, F., Kotrys, A. V., Zhan, Y., Artus-Revel, C.G., Eglinger, J., Stadler, M.B., Giorgetti, L. and Chao, J.A. (2017) The dynamics of mRNA turnover revealed by single-molecule imaging in single cells. *Mol. Cell*, **68**, 615–625.e9.
97. Pichon, X., Lagha, M., Mueller, F. and Bertrand, E. (2018) A growing toolbox to image gene expression in single cells: sensitive approaches for demanding challenges. *Mol. Cell*, **71**, 468–480.
98. Fusco, D., Accornero, N., Lavoie, B., Shenoy, S.M., Blanchard, J.M., Singer, R.H. and Bertrand, E. (2003) Single mRNA molecules demonstrate probabilistic movement in living mammalian cells. *Curr. Biol.*, **13**, 161–167.
99. Tutucci, E., Livingston, N.M., Singer, R.H. and Wu, B. (2018) Imaging mRNA in vivo, from birth to death. *Annu. Rev. Biophys.*, **47**, 85–106.
100. Autour, A., Jeng, S.C.Y., Cawte, A.D., Abdolhazadeh, A., Galli, A., Panchapakesan, S.S.S., Rueda, D., Ryckelynck, M. and Unrau, P.J. (2018) Fluorogenic RNA Mango aptamers for imaging small non-coding RNAs in mammalian cells. *Nat. Commun.*, **9**, 656.
101. Song, W., Filonov, G.S., Kim, H., Hirsch, M., Li, X., Moon, J.D. and Jaffrey, S.R. (2017) Imaging RNA polymerase III transcription using a photostable RNA-fluorophore complex. *Nat. Chem. Biol.*, **13**, 1187–1194.
102. Nelles, D.A., Fang, M.Y., O'Connell, M.R., Xu, J.L., Markmiller, S.J., Doudna, J.A. and Yeo, G.W. (2016) Programmable RNA tracking in live cells with CRISPR/Cas9. *Cell*, **165**, 488–496.

103. Cox, D.B.T., Gootenberg, J.S., Abudayyeh, O.O., Franklin, B., Kellner, M.J., Joung, J. and Zhang, F. (2017) RNA editing with CRISPR-Cas13. *Science (80-.)*, **358**, 1019–1027.
104. Wang, Y., Ni, T., Wang, W. and Liu, F. (2019) Gene transcription in bursting: a unified mode for realizing accuracy and stochasticity. *Biol. Rev.*, **94**, 248–258.
105. Larsson, A.J.M., Johnsson, P., Hagemann-Jensen, M., Hartmanis, L., Faridani, O.R., Reinius, B., Segerstolpe, Å., Rivera, C.M., Ren, B. and Sandberg, R. (2019) Genomic encoding of transcriptional burst kinetics. *Nature*, **565**, 251–254.
106. Liu, Z. and Tjian, R. (2018) Visualizing transcription factor dynamics in living cells. *J. Cell Biol.*, **217**, 1181–1191.
107. Nicolas, D., Phillips, N.E. and Naef, F. (2017) What shapes eukaryotic transcriptional bursting? *Mol. Biosyst.*, **13**, 1280–1290.
108. Patange, S., Girvan, M. and Larson, D.R. (2018) Single-cell systems biology: Probing the basic unit of information flow. *Curr. Opin. Syst. Biol.*, **8**, 7–15.
109. Symmons, O. and Raj, A. (2016) What's luck got to do with it: single cells, multiple fates, and biological nondeterminism. *Mol. Cell*, **62**, 788–802.
110. Neumann, F.R., Dion, V., Gehlen, L.R., Tsai-Pflugfelder, M., Schmid, R., Taddei, A. and Gasser, S.M. (2012) Targeted INO80 enhances subnuclear chromatin movement and ectopic homologous recombination. *Genes Dev.*, **26**, 369–383.
111. Shen, X., Mizuguchi, G., Hamiche, A. and Carl, W. (2000) A chromatin remodelling complex involved in transcription and DNA processing. *Nature*, **406**, 541–544.
112. Neely, K.E., Hassan, A.H., Wallberg, A.E., Steger, D.J., Cairns, B.R., Wright, A.P.H. and Workman, J.L. (1999) Activation domain-mediated targeting of the SWI/SNF complex to promoters stimulates transcription from nucleosome arrays. *Mol. Cell*, **4**, 649–655.
113. Gu, B., Swigut, T., Spencley, A., Bauer, M.R., Chung, M., Meyer, T. and Wysocka, J. (2018) Transcription-coupled changes in nuclear mobility of mammalian cis-regulatory elements. *Science*, **359**, 1050–1055.
114. Chen, H., Levo, M., Barinov, L., Fujioka, M., Jaynes, J.B. and Gregor, T. (2018) Dynamic interplay between enhancer–promoter topology and gene activity. *Nat. Genet.*, **50**, 1296–1303.
115. Bruinsma, R., Grosberg, A.Y., Rabin, Y. and Zidovska, A. (2014) Chromatin hydrodynamics. *Biophys. J.*, **106**, 1871–1881.
116. Nagashima, R., Hibino, K., Ashwin, S.S., Babokhov, M., Fujishiro, S., Imai, R., Nozaki, T., Tamura, S., Tani, T., Kimura, H. *et al.* (2019) Single nucleosome imaging reveals loose genome chromatin networks via active RNA polymerase II. *J. Cell Biol.*, **218**, 1511–1530.
117. Babokhov, M., Hibino, K., Itoh, Y. and Maeshima, K. (2019) Local chromatin motion and transcription. *J. Mol. Biol.*, **432**, 694–700.
118. Gribnau, J., De Boer, E., Trimborn, T., Wijgerde, M., Milot, E., Grosveld, F. and Fraser, P. (1998) Chromatin interaction mechanism of transcriptional control in vivo. *EMBO J.*, **17**, 6020–6027.
119. Cisse, I.I., Izeddin, I., Causse, S.Z., Boudarene, L., Senecal, A., Muresan, L., Dugast-Darzacq, C., Hajj, B., Dahan, M. and Darzacq, X. (2013) Real-time dynamics of RNA polymerase II clustering in live human cells. *Science*, **341**, 664–667.
120. Tinevez, J.Y., Perry, N., Schindelin, J., Hoopes, G.M., Reynolds, G.D., Laplantine, E., Bednarek, S.Y., Shorte, S.L. and Eliceiri, K.W. (2017) TrackMate: An open and extensible platform for single-particle tracking. *Methods*, **115**, 80–90.
121. Jaqaman, K., Loerke, D., Mettlen, M., Kuwata, H., Grinstein, S., Schmid, S.L. and Danuser, G. (2008) Robust single-particle tracking in live-cell time-lapse sequences. *Nat. Methods*, **5**, 695–702.
122. Lee, B.H. and Park, H.Y. (2018) HybTrack: A hybrid single particle tracking software using manual and automatic detection of dim signals. *Sci. Rep.*, **8**, 212.
123. Berg, S., Kutra, D., Kroeger, T., Straehle, C.N., Kausler, B.X., Haubold, C., Schiegg, M., Ales, J., Beier, T., Rudy, M. *et al.* (2019) ilastik: interactive machine learning for (bio)image analysis. *Nat. Methods*, **16**, 1226–1232.
124. Nozaki, T., Kaizu, K., Pack, C.G., Tamura, S., Tani, T., Hihara, S., Nagai, T., Takahashi, K. and Maeshima, K. (2013) Flexible and dynamic nucleosome fiber in living mammalian cells. *Nucl. (United States)*, **4**, 349–356.